COMMUNICATIONS PHYSICS

ARTICLE

DOI: 10.1038/s42005-018-0053-0 OPEN

Extreme-mass-ratio inspirals produced by tidal capture of binary black holes

Xian Chen [1,2] & Wen-Biao Han[3,4]

Extreme-mass-ratio inspirals (EMRIs) are important gravitational-wave (GW) sources for future space-based detectors. The standard model consists of one stellar-mass black hole spiraling into a supermassive one, and such a process emits low-frequency (~10^{-3} Hz) GWs, which contain rich information about the space–time geometry around the central massive body. Here we show that the small bodies in EMRIs, in fact, could be binary black holes, which are captured by the massive black holes during earlier close encounters. About 30% of the captured binaries coalesce due to the perturbation by the massive bodies, resulting in a merger rate of 0.03 $Gpc^3\,yr^{-1}$ in the most optimistic scenario. The coalescence generates also high-frequency (~10^2 Hz) GWs detectable by ground-based observatories, making these binary-EMRIs ideal targets for future multi-band GW observations.

[1] Astronomy Department, School of Physics, Peking University, 100871 Beijing, China. [2] Kavli Institute for Astronomy and Astrophysics at Peking University, 100871 Beijing, China. [3] Shanghai Astronomical Observatory, CAS, 200030 Shanghai, China. [4] School of Astronomy and Space Science, University of Chinese Academy of Sciences, Beijing 100049, China. Correspondence and requests for materials should be addressed to W.-B.H. (email: wbhan@shao.ac.cn)

An extreme-mass-ratio inspiral (EMRI) normally consists of a compact stellar object, such as a stellar-mass black hole (BH), and a supermassive black hole (SMBH). It is an important target for future space-borne, milli-Hz gravitational-wave (GW) detectors, such as the laser interferometer space antenna (LISA[1]): an EMRI could dwell in the LISA band for years[2–4], accumulating as many as 10^3–10^4 GW cycles in the data stream. Such a long waveform contains rich information about the space-time, as well as the astrophysical environment at the immediate exterior of a SMBH[5–7]. To decode this information, our model of an EMRI has to be highly accurate, both mathematically and physically.

In the canonical model of an EMRI, the stellar object is captured by the SMBH in two possible ways[3]: (i) it is scattered by other stars, a process known as relaxation, to such a small distance to the SMBH that the stellar object loses a significant amount of its orbital energy through GW radiation and becomes bound to the big BH[8,9]. The event rate of this type of EMRIs is difficult to estimate because it depends on factors that are poorly constrained by observations. The current estimation lies in a broad range between 10^{-9} and 10^{-6} per galaxy per year[4,10–15]; (ii) the small body could come from a binary which is also scattered to the vicinity of the SMBH. If the distance between the SMBH and the centre-of-mass of the binary becomes smaller than the tidal radius, $R_t \equiv a(M_3/m_{12})^{1/3}$, where a and m_{12} are the semi-major axis and total mass of the binary and M_3 the mass of the SMBH, the interaction in general ejects the lighter member of the binary and leaves the other, more massive member on a bound orbit around the SMBH[16–18]. The corresponding event rate could be comparable to that produced by the aforementioned capture of individual BHs from eccentric orbits[18].

In this article, we point to a third possibility. We show that a BH binary (BHB) could be tidally captured by a SMBH to a bound orbit. This could happen when the binary passes by the SMBH at such a close distance that the tidal interaction transforms a fraction of the kinetic energy into the internal potential energy of the binary[17,19]. We refer to the resulting triple system as the "binary EMRI" (b-EMRI) and investigate its long-term evolution using numerical simulations. We find that the captured binary, as a single unit, could survive around the SMBH for a long time. A significant fraction of the BHBs coalesce before their orbits around the SMBHs completely circularize. The result could be a burst of high-frequency (10^2 Hz) GWs happening at the same time and in the same sky position of a low-frequency (10^{-3} Hz) EMRI.

Results

Formation of a b-EMRI. Our BHB starts most likely around the influence radius of the SMBH, $R_{\rm inf} \equiv GM_3/\sigma^2$, where σ is the one-dimensional velocity dispersion of the stars surrounding the SMBH (or "nuclear star cluster", NSC[20]). Deeper inside this radius the BHB is susceptible to ionization by energetic encounters with interlopers[21,22] and further outside the gravitational influence of the SMBH becomes negligible. Using the typical values $M_3 = 10^6 M_\odot$ and $\sigma = 60$ km s^{-1} for NSCs, we find $R_{\rm inf} \simeq 1$ pc.

Because the specific energy of the BHB initially is $3\sigma^2/2 - GM_3/R_{\rm inf} = \sigma^2/2$, the orbit is a hyperbola with an asymptotic velocity of $v_0 = \sigma$ at infinity. Previous studies focus on parabolic orbits[19] and have shown that tidal capture happens when the pericentre distance of the parabola, R_p, becomes comparable to the tidal radius R_t, i.e.,

$$R_p \simeq \xi R_t \simeq 74 R_g \left(\frac{\xi}{2}\right)\left(\frac{a}{10^5 r_g}\right) \times \left(\frac{2}{1+q}\right)^{1/3}\left(\frac{m_1}{10M_\odot}\right)^{2/3}\left(\frac{M_3}{10^6 M_\odot}\right)^{-2/3}, \quad (1)$$

where $1 \lesssim \xi \lesssim 5$. In the last equation, $R_g = GM_3/c^2$ is the gravitational radius of the SMBH, c is the speed of light, m_1 and m_2 are the masses of the two stellar BHs, $q \equiv m_2/m_1$ is the mass ratio assuming that $m_1 \geq m_2$, and $r_g = Gm_1/c^2$ is the gravitational radius of the bigger stellar BH. In the following we assume $q \simeq 1$ because star clusters produce, most likely, equal-mass binaries[23–25]. We also scale a with $10^5 r_g$ and the reason will become clear later. The lifetime of these BHBs can been calculated in the Keplerian approximation[26],

$$t_{\rm gw}(a,e) = \frac{a}{4|\dot{a}|} = \frac{5a^4 F(e)}{256 c r_g^3 q(1+q)} \quad (2)$$

$$\simeq \frac{3.1\times 10^6}{q(1+q)}\left(\frac{m_1}{10M_\odot}\right)\left(\frac{a}{10^5 r_g}\right)^4 F(e)\,\text{years}, \quad (3)$$

where $\dot{a}$ is the decay rate of the semi-major axis due to GW radiation, e is the orbital eccentricity, and $F(e) = (1-e^2)^{7/2}(1 + 73e^2/24 + 37e^4/96)^{-1}$.

To prove that the above criterion for tidal capture also applies to hyperbolic orbits, we conduct scattering experiments using the numerical tool FEWBODY[27]. The default parameters are $M_3 = 10^6 M_\odot$, $m_1 = m_2 = 10M_\odot$, $e = 0.1$, and $a_0 = 5\times 10^4 r_g \simeq 0.005$ AU. Initially we place the BHB at infinity with a velocity of $v_0 = 60$ km s^{-1}. The direction of the velocity is chosen in such a way that the hyperbolic orbit initially has a pericentre distance of ξR_t. We then numerically integrate the triple system and, after the first pericentre passage, record the relative energy change of the BHB, $\eta \equiv (E - E_0)/|E_0|$, where E is the final energy of the BHB and $E_0 = -Gm_1m_2/(2a_0)$ is the initial energy.

If $\eta \geq 1$, the binary is tidally disrupted. Otherwise, the binary survives the pericentre passage. Since the BHB initially has a kinetic energy of $K_0 = m_{12}v_0^2/2$, we know that the binary becomes bound to the SMBH if $E - E_0 > K_0$, i.e., $\eta \gtrsim a_0 v_0^2/(G\mu) \simeq 0.0041$, where $\mu = m_1m_2/m_{12}$ is the reduced mass of the binary. If $\eta < 0.0041$, the BHB is re-ejected to infinity. Figure 1 shows the cumulative distribution of η for different ξ, where we have randomized the initial inclination of the BHB and repeated the experiment 10^3 times for each value of ξ. We find that the captured fraction is $f_{\rm cap} = (10$–$30)\%$ when ξ varies between 0.7 and 2.5. Therefore, b-EMRIs can form via capturing the BHBs on hyperbolic orbits.

The orbital elements of the b-EMRIs can be derived from two conservation laws: (i) because of the conservation of energy, the binding energy (relative to the SMBH) of a captured BHB is $E_3 = K_0 - \eta|E_0| \simeq \eta Gm_1m_2/(2a_0)$, where the last approximation uses the previous result that $\eta \sim 0.1$. From E_3 we derive a semi-major axis of $R \simeq (a_0/\eta)(M_3/\mu)$. (ii) The pericentre remains to be R_p because of the conservation of angular momentum. Consequently, the eccentricity e_3 satisfies the condition

$$1 - e_3 = \frac{R_p}{R} \simeq 9.3\times 10^{-5}\frac{q}{(1+q)^{4/3}}\left(\frac{\xi}{2}\right)\times\left(\frac{\eta}{0.1}\right)\left(\frac{m_1}{10M_\odot}\right)^{2/3}\left(\frac{M_3}{10^6 M_\odot}\right)^{-2/3}. \quad (4)$$

Interestingly, it does not depend on our assumption of a_0. The small value of $1 - e_3$ indicates that a newly formed b-EMRI, in general, is very eccentric.

The high eccentricity will affect the stability of a b-EMRI in two ways. On the one hand, the orbital motion of the BHB around the SMBH is more susceptible to perturbations by the surrounding stars because the angular momentum, $\sqrt{GM_3R(1-e_3^2)}$, is small. To be more quantitative, suppose $T_{\rm rlx}$ characterizes the typical timescale for stellar relaxation processes to completely alter the orbital elements of a circular orbit[3], the timescale to spoil an orbit

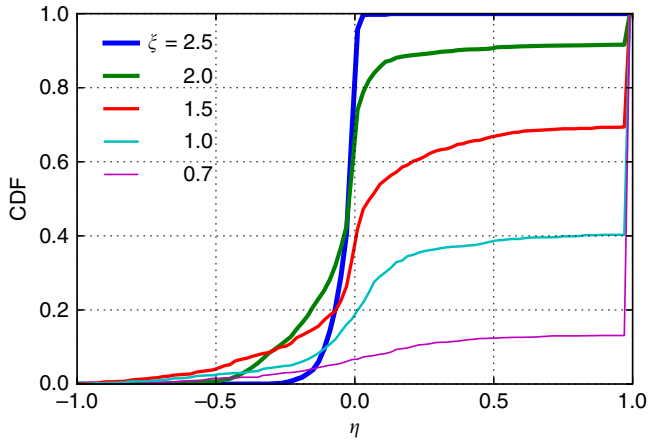

Fig. 1 Cumulative distribution function of the η parameter. This parameter characterizes the relative energy change of a black hole binary (BHB) during its first pericentre passage of a hyperbolic orbit. The curves with different thickness refer to simulations with different ξ factors. In our model, tidal captures fall in the interval of $0.0041 < \eta < 0.95$

of an eccentricity of e_3 is only $T_{\rm rlx}\left(1-e_3^2\right)$. On the other hand, the orbit circularizes very fast due to GW radiation because the associated timescale $T_{\rm gw}$ (during which $1-e_3$ increases) is proportional to $R^4\left(1-e_3^2\right)^{7/2}$. For our purpose, we use the relationship $R_{\rm p}=R(1-e_3)$ to rewrite $T_{\rm gw}$ and find that

$$T_{\rm gw} \simeq 15R_{\rm p}^4\, 256\, c\, R_{\rm g}^3\left(\frac{M_3}{m_{12}}\right)(1-e_3)^{-1/2} \simeq 1.2\times 10^6\left(\frac{1+q}{2}\right)^{-7/3}\left(\frac{\xi}{2}\right)^4\left(\frac{1-e_3}{10^{-4}}\right)^{-1/2} \quad (5)$$

$$\times\left(\frac{m_1}{10\,M_\odot}\right)^{5/3}\left(\frac{M_3}{10^6\,M_\odot}\right)^{-2/3}\left(\frac{a}{10^5\,r_{\rm g}}\right)^4 \text{years}. \quad (6)$$

Based on the understanding of the above two effects, we find that the b-EMRIs with $\left(1-e_3^2\right)T_{\rm rlx}>T_{\rm gw}$ are not any more affected by the relaxation of the background stars. Together with Eqs. (4) and (6), we find that these "clean" b-EMRIs satisfy

$$a<a_{\rm cri} \simeq 4.2\times 10^4\, r_{\rm g}\frac{q^{3/8}}{(1+q)^{-1/12}}\left(\frac{T_{\rm rlx}}{10^9\,\text{years}}\right)^{1/4}\left(\frac{\xi}{2}\right)^{-5/8} \times\left(\frac{\eta}{0.1}\right)^{3/8}\left(\frac{m_1}{10M_\odot}\right)^{-1/6}\left(\frac{M_3}{10^6\,M_\odot}\right)^{-1/12}. \quad (7)$$

This is the reason that we scaled a with $10^5 r_{\rm g}$ in the previous equations. In the last equation we have adopted a typical value of 10^9 years for $T_{\rm rlx}$. We choose this value because our b-EMRI resides in the phase space of $(1-e_3)\sim 10^{-4}$ and $R=R_{\rm p}/(1-e_3)\sim 0.02$ pc (assuming $a=a_{\rm cri}$), a region where two-body scattering dominates the relaxation process[28,29].

Long-term evolution. Although the long-term interaction between a SMBH and a binary has been studied previously[21,30–37], these earlier works focus on a binary that is far away from the SMBH, so that there is no energy exchange between the "inner binary", i.e., the BHB, and the "outer binary", i.e. the pair formed by the BHB and the SMBH. Such triple systems are called "hierarchical triples". Moreover, because of the large distance, the GW radiation of the outer binary is also unimportant to the overall dynamics. Under these circumstances, the evolution reduces to a periodic oscillation of the inner binary in the eccentricity space, which is known as the "Lidov–Kozai" cycle[38,39]. In our problem, however, the BHB is much closer to the SMBH so that the energies of the inner and outer binaries are no longer conserved and the GW radiation from the outer binary is not negligible. These are the key differences between our problem and other studies.

The b-EMRIs, in general, do not satisfy the criterion of hierarchical triple. In our problem, since $M/m_{12}\gg 1$ and $1+e_3\simeq 2$, the criterion for hierarchical triple[40] reduces to

$$\frac{R_{\rm p}}{R_{\rm t}}\gtrsim 23\left(\frac{1-e_3}{10^{-4}}\right)^{-1/5}\left(\frac{M_3}{m_{12}}\right)^{1/15}. \quad (8)$$

Our b-EMRIs do not satisfy this condition because tidal capture requires that $1\lesssim R_{\rm p}/R_{\rm t}\lesssim 2.5$ (see Fig. 1). For this reason, we use again Fewbody to evolve the triple system numerically. Besides adopting the default parameters, we also choose $\xi=2$ and $1-e_3=10^{-4}$ as the initial conditions and start the BHB at the apocentre with a random inclination.

Moreover, we notice that $T_{\rm gw}$ is of the same order of $t_{\rm gw}$. If the eccentricity of the inner binary gets excited by the tidal force of the SMBH, the BHB may coalesce. This would terminate the b-EMRI. To include this effect in the simulation, we implement post-Newtonian (PN) corrections to the equations of motion of the inner binary, as has been done by one of the authors in a previous work[24]. Figure 2 shows an example of a coalescence. It also shows that the energy of the inner binary is not conserved, confirming our prediction that the system is not a hierarchical triple.

With the above setup, we run 10^4 simulations to get reasonable statistics. Figure 3 summarizes the outcomes. Interestingly, in about 30% of the cases, the BHBs coalesce well before the time limit $t=T_{\rm gw}/2$ (for circularization) is reached. Because coalescing BHBs generate high-frequency GWs (10^2 Hz) and their orbital motion around the SMBH produces low-frequency ones (10^{-3} Hz), we conclude that b-EMRIs, in principle, could be detected by both ground-based and space-based detectors. Figure 4 illustrates this idea and we will elaborate this point in Discussion.

Furthermore, about 0.6% of our b-EMRIs survive till the time $t=T_{\rm gw}/2$. In principle they could have significantly circularized, i.e., both the semi-major axis R and the eccentricity e_3 of the outer binary could have significantly decreased. However, our code does not include PN corrections to the outer binary and this shortcoming prevents us from predicting the fate of these long-lived b-EMRIs. One way of circumventing this issue is to repeat our b-EMRI simulations with smaller e, i.e., $e=0.999$ or 0.99, to mimic the process of circularization, but the integration time exceeds our current computational capacity. We plan to resolve this issue in a future work. We note that PN corrections would not significantly affect the previous results about the capturing process because during the first periapsis passage the periastron shift, which is of the order of $2R_{\rm g}/R_{\rm p}\sim 0.027$, is small and the energy lost via GW radiation is negligible relative to the dynamical energy exchange $|E-E_0|$.

Formation rate. The formation rate of b-EMRIs can be estimated with $\Gamma=pf_{\rm cap}\Gamma_{\rm BHB}$. Here $\Gamma_{\rm BHB}$ denotes the formation rate of the BHBs with $a\simeq a_{\rm cri}$ in NSCs, p is the probability that such a BHB is on a hyperbolic orbit with $\xi\lesssim 2$, and $f_{\rm cap}\simeq 0.3$ is the probability for capture (from Fig. 1).

To quantify $\Gamma_{\rm BHB}$, we notice that the BHBs of our interest are short-lived (see Eq. (3)) relative to the age of a galaxy, which is about 10^{10} years. Therefore, $\Gamma_{\rm BHB}$ is equal to the event rate of BHB mergers in a galaxy. Recent calculations[22,41] suggest that

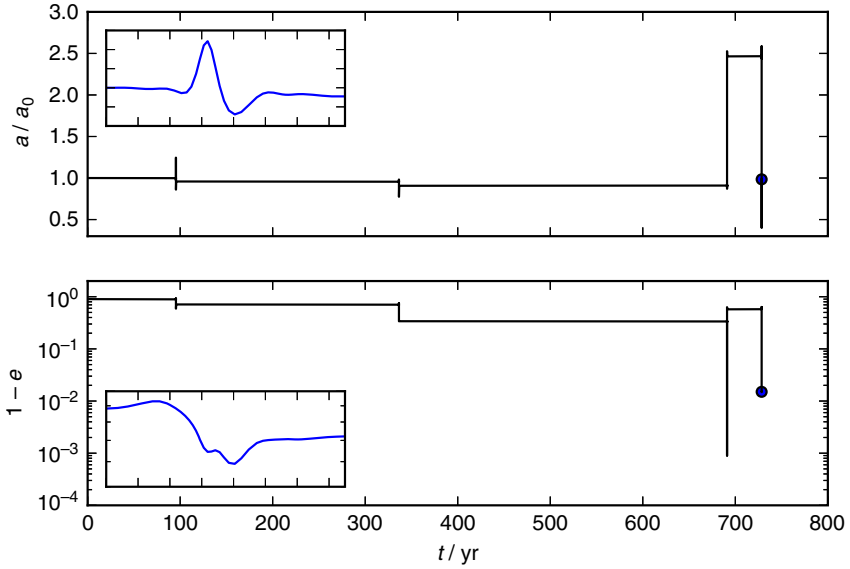

Fig. 2 An example showing the evolution of the semi-major axis and eccentricity of the inner black hole binary (BHB). The discontinuities coincide with the pericentre passages. The black dot at the end of each curve marks the final output of the code, where the BHB has passed the pericentre and is $10^3 R_t$ away from the supermassive black hole (SMBH). At this moment t_{gw} is only 35 days so that the BHB will coalesce shortly afterwards. The intersecting plot in each panel shows a close-up of the evolution of about one hour during the first pericentre passage

$\Gamma_{\rm BHB} \sim$ few $\times 10^{-7}$ galaxy^{-1} year^{-1}. This rate dose not account for the enhancement due to the interaction between BHBs and SMBHs[21]. When this enhancement is considered, the rate could be as high as $\Gamma_{\rm BHB} = (0.8-2)\times 10^{-6}$ galaxy^{-1} year^{-1} according to the most optimistic estimations[33,35].

To quantify p, we first recall that our BHBs start from a rather large distance, $R_{\rm inf}$, from the SMBH, where the binaries have a maximum angular momentum of $L_c \simeq \sqrt{GM_3R_{\rm inf}}$ (i.e., the angular momentum for a circular orbit of the same energy). To reach a pericentre distance of $R_{\rm p}$, the BHBs would have to diffuse in the angular-momentum space (L-space) due to relaxation to reach a region where $L \lesssim L_{\rm p} \sim \sqrt{2GM_3R_{\rm p}}$. If the relaxation process is incoherent[42], like the aforementioned two-body relaxation, the probability that the BHB appears at $L \lesssim L_{\rm p}$ is proportional to L^2. With this consideration and assuming $a_{\rm cri} = 5\times 10^4 r_{\rm g}$, we derive $p \simeq (L_{\rm p}/L_{\rm c})^2 \simeq 4\times 10^{-6}$. Such a small probability renders the b-EMRI rate formidably small, i.e. $\Gamma \sim (10^{-12}$–$10^{-11})$ galaxy^{-1} year^{-1}.

However, if the relaxation process is coherent, e.g., due to a massive perturber or an axisymmetric gravitational potential[43–46], the probability p scales with L, so that $p \simeq L_{\rm p}/L_{\rm c} \simeq 2\times 10^{-3}$. With this number, we find Γ ranges from 10^{-10} galaxy^{-1} year^{-1} to as large as few $\times 10^{-9}$ galaxy^{-1} year^{-1} in the most optimistic estimation. These numbers should be regarded as upper limits because the coherent relaxation processes normally affect only part of the angular-momentum space so that the real value of p could be significantly smaller than $L_{\rm p}/L_{\rm c}$.

Comparing these rates with the event rate of standard EMRIs[4,10–15], which falls in the range of 10^{-9}–10^{-6} yr^{-1} galaxy^{-1}, we conclude that in the most optimistic case the b-EMRI rate could approach the lower boundary of the EMRI rate. Furthermore, since there are on average 2×10^7 galaxies per Gpc^3 (earlier studies[41] use the same galaxy density), we finally find that the above formation rate of b-EMRIs is equivalent to $(10^{-5}$–$10^{-4})$ Gpc^3 year^{-1} in the pessimistic case and 0.1 Gpc^3 year^{-1} in the most optimistic one.

Although the formation rate is relatively low, each b-EMRI has a non-negligible lifetime. The extended lifetime leads to a substantial duty cycle, $D_{\rm bemri}$, for a galaxy to host a b-EMRI. To estimate $D_{\rm bemri}$, we use (i) the formation rate Γ and (ii) the probability of surviving b-EMRIs as a function of time, $f_{\rm bemri}(t)$, which is shown in Fig. 3 as the black solid curve, to derive $D_{\rm bemri} \simeq \Gamma t f_{\rm bemri}(t)$. In the previous equation, the maximum value of $tf_{\rm bemri}(t)$ appears at $t \simeq 7600$ years, where $f_{\rm bemri}(t) \simeq 0.1$. Therefore, we find that $D_{\rm bemri} \simeq (10^{-9}$–$10^{-8})$ galaxy^{-1} in our pessimistic scenario and $D_{\rm bemri} \sim 10^{-6}$ galaxy^{-1} in the most optimistic one. This result means that within a volume of 1 Gpc^3 (corresponding to a distance of about 600 Mpc), there are, on average, $N_{\rm bemri} \sim 0.02$–20 b-EMRIs.

Discussion

We have seen that the BHBs in b-EMRIs, in general, have $a \lesssim a_{\rm cri}$. Interestingly, these BHBs are detectable by LISA. This is so because LISA is sensitive to the GWs with a frequency of $f \sim 10^{-3}$ Hz and the strongest GW mode that a BHB emits[47,48] is of a frequency of $f \simeq \pi^{-1}\sqrt{Gm_{12}/[a(1-e)]^3}$. As a result, those BHBs with a semi-major axis of

$$a_{\rm LISA} \sim 3.4\times 10^4\, r_{\rm g} f_{-3}^{-2/3} \frac{(1+q)^{1/3}}{1-e}\left(\frac{m_1}{10M_\odot}\right)^{-2/3} \qquad (9)$$

are inside the LISA band, where $f_{-3} := f/(10^{-3}\,{\rm Hz})$. This critical semi-major axis is comparable to $a_{\rm cri}$.

It is important to note that the BHBs in b-EMRIs are accelerating in the gravitational potential of the SMBHs. This condition could induce detectable shift to the phase of the GW inspiral waveform[49,50]. We have seen that within a distance of about 600 Mpc there are at most 20 accelerating BHBs for LISA to detect. In our default model, the BHB is at a typical distance of $R \simeq 0.02$ pc from the central SMBH. The corresponding acceleration is GM_3/R^2 and it could induce a phase shift as large as $10^3\pi$ per year according to the formula derived in the earlier studies[49,50].

Furthermore, the orbital motion of the BHBs around the SMBHs also generates GWs. It is important to understand whether this radiation is detectable. Similar to the previous analysis

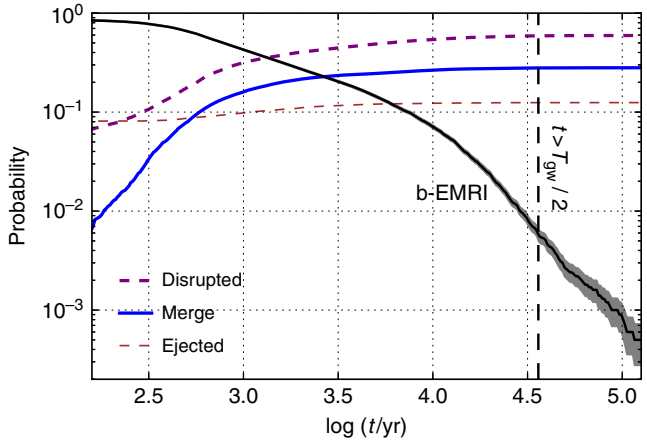

Fig. 3 Probabilities as a function of time for the following four outcomes. First, the black hole binary (BHB) in the binary extrme-mass-ratio inspiral (b-EMRI) remains bound to the supermassive black hole (SMBH) (black solid line). The grey shaded area correspond to the statistical Poisson error, calculated with the square root of the number of experiments. Second, the BHB is disrupted by the tidal force of the SMBH (thick dashed curve). Third, the BHB is ejected to infinity (thin dashed curve). Fourth, the BHB coalesces into a single black hole (blue solid curve). The vertical dashed line indicates half of the gravitational wave (GW) radiation timescale $T_{\rm gw}/2$ of a typical b-EMRI with $\xi = 2$ and $1 - e_3 = 10^{-4}$. Beyond this time, the BHB would circularize around the BHB due to GW radiation but our code cannot capture this feature

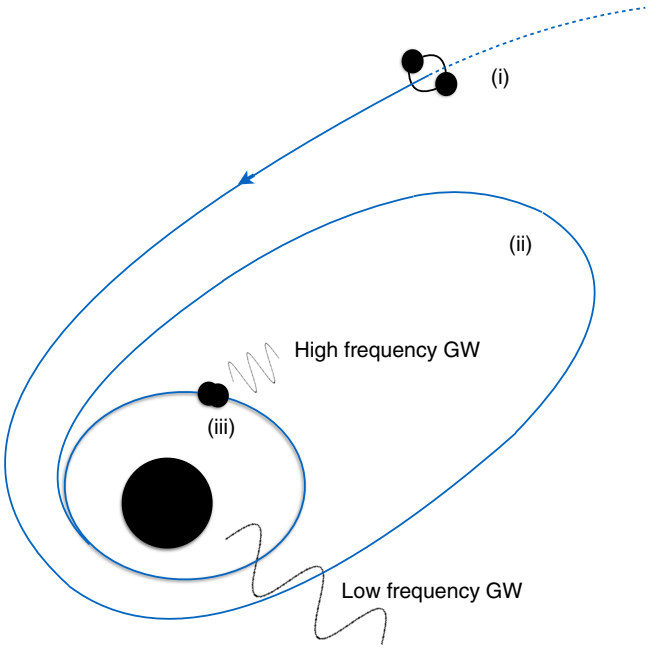

Fig. 4 Three evolutionary stages of a binary extrme-mass-ratio inspiral (b-EMRI). First, in (i), a compact black hole binary (BHB) is captured to a bound orbit around a supermassive black hole (SMBH) because the pericentre distance becomes comparable to the tidal-disruption radius, $R_{\rm t}$. Next, in (ii), the outer binary circularizes due to gravitational wave (GW) radiation, and the GW frequency lies in the band of a space-borne GW detector. Finally, in (iii), the tidal force of the SMBH becomes strong enough to excite the eccentricity of the inner BHB and drive it to merge. The merger produces high-frequency GWs

for BHBs, we calculate the frequency of the strongest GW mode as $f = \pi^{-1}\sqrt{GM_3/R_{\rm p}^3}$, so that a b-EMRI is inside the LISA band if its periapsis is

$$R_{\rm p} \sim R_{\rm LISA} \simeq 16 R_{\rm g} f_{-3}^{-2/3} M_6^{-2/3}. \quad (10)$$

From Eqs. (1) and (7), we find that our b-EMRIs satisfy the condition

$$R_{\rm p} \lesssim 24 R_{\rm g} \frac{(q\xi)^{3/8}}{(1+q)^{1/4}} \left(\frac{T_{\rm rlx}}{10^9\,{\rm yr}}\right)^{1/4} \times \left(\frac{\eta}{0.1}\right)^{3/8} \left(\frac{m_1}{10 M_\odot}\right)^{1/2} \left(\frac{M_3}{10^6 M_\odot}\right)^{-3/4}. \quad (11)$$

Therefore, they are indeed inside the LISA band: Each pericentre passage will generate a burst of GWs detectable by LISA[51–54].

These b-EMRIs are particularly interesting from the observational point of view because they generate two types of GWs, i.e., the continuous waves from the BHBs and bursts from the orbital motion of the BHBs around the SMBHs. Moreover, the two types of GWs are emitted at the same time in the same band. LISA can detect a single burst of the second type out to a distance of about $200(m_{12}/20\ M_\odot)$ Mpc[52]. If the BHB has a total mass of about $60 M_\odot$, like what the Laser Interferometer Gravitational-wave Observatory (LIGO) first detected[23], the detection horizon would become as far as 600 Mpc. We already know that there are at most $N_{\rm bemri} \simeq 20$ b-EMRIs within this distance. Now we estimate the chance of catching a GW burst at the moment of the pericentre passage. Since the majority of the b-EMRIs cannot circularize (see Fig. 3), the successive pericentre passages are separated by a long orbital period of the outer binary, which is about $P_3 \simeq$ 200 years in our fiducial model. Given that LISA is designed to have a mission duration of $\Delta t = 5$ years[1], the chance of catching a b-EMRI at its pericentre passage is about $(\Delta t/P)N_{\rm bemri} \sim 50\%$ in our most optimistic scenario.

Probably the most interesting feature about b-EMRIs is that the BHBs have a 30% chance to coalesce. The coalescence gives rise to a LIGO/Virgo event. The event rate is 0.3Γ, which is 0.03 Gpc^3 year^{-1} in the most optimistic scenario and two orders of magnitude smaller in the most pessimistic one. If detected, the LIGO/Virgo event is likely separated from a LISA event, i.e., the GW burst generated during the pericentre passage, by about half of the orbital period of the outer binary, or 100 years in our fiducial model, because the coalescence happens most likely at the apocentre where the passing time is the longest. For this reason, it would be difficult to identify the LISA counterpart to the LIGO/Virgo event.

However, exceptions might exist. If the BHB in a b-EMRI could circularize around the SMBH, the orbital period P_3 would be much shorter and hence the LISA and LIGO/Virgo events would appear much closer in time. According to our calculation, the event rate of such an exceptional case is at most $\Gamma f_{\rm bemri}(t = T_{\rm gw}/2) \sim 6 \times 10^{-4}$ Gpc^3 year^{-1}.

In summary, we have shown that the small bodies in EMRIs could, in fact, be BH binaries. Such b-EMRIs could form via tidal capture and a significant fraction of the captured BHBs could merge due to the perturbation by the SMBHs. Although rare, they are ideal targets for future multi-band GW observations[55,56]. First, the merger generates high-frequency GWs, i.e. a LIGO/Virgo event that is in the same sky location of a LISA EMRI event. Second, the high-frequency GWs could be redshifted because they are generated very close to a SMBH[57], providing a rare opportunity of studying the propagation of GWs in the regime of strong gravity. Third, the merger also induces a kick to the BH remnant[58]. This kick causes a glitch in the EMRI waveform, which, through a careful analysis, is discernible in the data stream[59].

Data availability

The data sets generated during the current study are available from the corresponding author on reasonable request.

Received: 27 January 2018 Accepted: 16 August 2018
Published online: 10 September 2018

References

1. Amaro-Seoane, P. et al. Laser interferometer space antenna. Preprint at http://arxiv.org/abs/1702.00786 (2017).
2. Barack, L. & Cutler, C. LISA capture sources: approximate waveforms, signal-to-noise ratios, and parameter estimation accuracy. *Phys. Rev. D.* **69**, 082005 (2004).
3. Amaro-Seoane, P. et al. TOPICAL REVIEW: intermediate and extreme mass-ratio inspirals-astrophysics, science applications and detection using LISA. *Class. Quantum Gravity* **24**, R113–R169 (2007).
4. Babak, S. et al. Science with the space-based interferometer LISA. V. Extreme mass-ratio inspirals. *Phys. Rev. D* **95**, 103012 (2017).
5. Kocsis, B., Yunes, N. & Loeb, A. Observable signatures of extreme mass-ratio inspiral black hole binaries embedded in thin accretion disks. *Phys. Rev. D* **84**, 024032 (2011).
6. Gair, J. R., Vallisneri, M., Larson, S. L. & Baker, J. G. Testing general relativity with low-frequency, space-based gravitational-wave detectors. *Living Rev. Relativ.* **16**, 7 (2013).
7. Barausse, E., Cardoso, V. & Pani, P. Can environmental effects spoil precision gravitational-wave astrophysics? *Phys. Rev. D* **89**, 104059 (2014).
8. Hils, D. & Bender, P. L. Gradual approach to coalescence for compact stars orbiting massive black holes. *Astrophys. J. Lett.* **445**, L7–L10 (1995).
9. Sigurdsson, S. & Rees, M. J. Capture of stellar mass compact objects by massive black holes in galactic cusps. *Mon. Not. R. Astron. Soc.* **284**, 318–326 (1997).
10. Freitag, M. Monte Carlo cluster simulations to determine the rate of compact star inspiralling to a central galactic black hole. *Class. Quantum Gravity* **18**, 4033–4038 (2001).
11. Hopman, C. & Alexander, T. The orbital statistics of stellar inspiral and relaxation near a massive black hole: characterizing gravitational wave sources. *Astrophys. J.* **629**, 362–372 (2005).
12. Hopman, C. Binary dynamics near a massive black hole. *Astrophys. J.* **700**, 1933–1951 (2009).
13. Amaro-Seoane, P. & Preto, M. The impact of realistic models of mass segregation on the event rate of extreme-mass ratio inspirals and cusp re-growth. *Class. Quantum Gravity* **28**, 094017 (2011).
14. Aharon, D., & Perets, H. B. The impact of mass segregation and star formation on the rates of gravitational-wave sources from extreme mass ratio inspirals. *Astrophys. J. Lett.* **830**, L1 (2016).
15. Bar-Or, B. & Alexander, T. Steady-state relativistic stellar dynamics around a massive black hole. *Astrophys. J.* **820**, 129 (2016).
16. Hills, J. G. Hyper-velocity and tidal stars from binaries disrupted by a massive galactic black hole. *Nature* **331**, 687–689 (1988).
17. Hills, J. G. Computer simulations of encounters between massive black holes and binaries. *Astron. J.* **102**, 704–715 (1991).
18. Miller, M. C., Freitag, M., Hamilton, D. P. & Lauburg, V. M. Binary encounters with supermassive black holes: zero-eccentricity LISA events. *Astrophys. J. Lett.* **631**, L117–L120 (2005).
19. Addison, E., Laguna, P. & Larson, S. Busting up binaries: encounters between compact binaries and a supermassive black hole. Preprint at Preprint at http://arxiv.org/abs/1501.07856 (2015).
20. Tremaine, S. et al. The slope of the black hole mass versus velocity dispersion correlation. *Astrophys. J.* **574**, 740–753 (2002).
21. Antonini, F. & Perets, H. B. Secular evolution of compact binaries near massive black holes: gravitational wave sources and other exotica. *Astrophys. J.* **757**, 27 (2012).
22. Leigh, N. W. C. et al. On the rate of black hole binary mergers in galactic nuclei due to dynamical hardening. *Mon. Not. R. Astron. Soc.* **474**, 5672–5683 (2018).
23. Abbott, B. P. et al. Astrophysical Implications of the Binary Black-hole Merger GW150914. *Astrophys. J. Lett.* **818**, L22 (2016).
24. Amaro-Seoane, P. & Chen, X. Relativistic mergers of black hole binaries have large, similar masses, low spins and are circular. *Mon. Not. R. Astron. Soc.* **458**, 3075–3082 (2016).
25. O'Leary, R. M., Meiron, Y. & Kocsis, B. Dynamical formation signatures of black hole binaries in the first detected mergers by LIGO. *Astrophys. J. Lett.* **824**, L12 (2016).
26. Peters, P. C. Gravitational radiation and the motion of two point masses. *Phys. Rev.* **136**, 1224–1232 (1964).
27. Fregeau, J. M., Cheung, P., Portegies Zwart, S. F. & Rasio, F. A. Stellar collisions during binary-binary and binary-single star interactions. *Mon. Not. R. Astron. Soc.* **352**, 1–19 (2004).
28. Merritt, D., Alexander, T., Mikkola, S. & Will, C. M. Stellar dynamics of extreme-mass-ratio inspirals. *Phys. Rev. D.* **84**, 044024 (2011).
29. Alexander, T. Stellar dynamics and stellar phenomena near a massive black hole. *Annu. Rev. Astron. Astrophys.* **55**, 17–57 (2017).
30. Mandel, I. & Levin, Y. Double tidal disruptions in galactic nuclei. *Astrophys. J. Lett.* **805**, L4 (2015).
31. Prodan, S., Antonini, F. & Perets, H. B. Secular evolution of binaries near massive black holes: formation of compact binaries, merger/collision products and G2-like objects. *Astrophys. J.* **799**, 118 (2015).
32. Stephan, A. P. et al. Merging binaries in the Galactic Center: the eccentric Kozai-Lidov mechanism with stellar evolution. *Mon. Not. R. Astron. Soc.* **460**, 3494–3504 (2016).
33. VanLandingham, J. H., Miller, M. C., Hamilton, D. P. & Richardson, D. C. The role of the Kozai-Lidov mechanism in black hole binary mergers in Galactic Centers. *Astrophys. J.* **828**, 77 (2016).
34. Liu, B., Wang, Y.-H. & Yuan, Y.-F. Modified evolution of stellar binaries from supermassive black hole binaries. *Mon. Not. R. Astron. Soc.* **466**, 3376–3386 (2017).
35. Petrovich, C. & Antonini, F. Greatly enhanced merger rates of compact-object binaries in non-spherical nuclear star clusters. *Astrophys. J.* **846**, 146 (2017).
36. Bradnick, B., Mandel, I. & Levin, Y. Stellar binaries in galactic nuclei: tidally stimulated mergers followed by tidal disruptions. *Mon. Not. R. Astron. Soc.* **469**, 2042–2048 (2017).
37. Hoang, B.-M., Naoz, S., Kocsis, B., Rasio, F. A. & Dosopoulou, F. Black hole mergers in galactic nuclei induced by the eccentric Kozai–Lidov effect. *Astrophys. J.* **856**, 140 (2018).
38. Lidov, M. L. The evolution of orbits of artificial satellites of planets under the action of gravitational perturbations of external bodies. *Planet. Space Sci.* **9**, 719–759 (1962).
39. Kozai, Y. Secular perturbations of asteroids with high inclination and eccentricity. *AJ* **67**, 591–598 (1962).
40. Mardling, R. A. & Aarseth, S. J. Tidal interactions in star cluster simulations. *Mon. Not. R. Astron. Soc.* **321**, 398–420 (2001).
41. Antonini, F. & Rasio, F. A. Merging black hole binaries in Galactic Nuclei: implications for advanced-LIGO detections. *Astrophys. J.* **831**, 187 (2016).
42. Binney, J. & Tremaine, S. *Galactic Dynamics*. 2nd edn (Princeton University Press: Princeton, NJ, USA, 2008).
43. Perets, H. B., Hopman, C. & Alexander, T. Massive perturber-driven interactions between stars and a massive black hole. *Astrophys. J.* **656**, 709–720 (2007).
44. Chen, X., Sesana, A., Madau, P. & Liu, F. K. Tidal stellar disruptions by massive black hole pairs. II. Decaying binaries. *Astrophys. J.* **729**, 13 (2011).
45. Chen, X. & Liu, F. K. Is there an intermediate massive black hole in the Galactic Center: imprints on the stellar tidal-disruption rate. *Astrophys. J.* **762**, 95 (2013).
46. Chen, X. & Amaro-Seoane, P. A rapidly evolving region in the Galactic Center: why S-stars thermalize and more massive stars are missing. *Astrophys. J. Lett.* **786**, L14 (2014).
47. Farmer, A. J. & Phinney, E. S. The gravitational wave background from cosmological compact binaries. *Mon. Not. R. Astron. Soc.* **346**, 1197–1214 (2003).
48. Wen, L. On the eccentricity distribution of coalescing black hole binaries driven by the Kozai mechanism in globular clusters. *Astrophys. J.* **598**, 419–430 (2003).
49. Inayoshi, K., Haiman, Z. & Ostriker, J. P. Hyper–Eddington accretion flows on to massive black holes. *Mon. Not. R. Astron. Soc.* **459**, 3738–3755 (2016).
50. Meiron, Y., Kocsis, B. & Loeb, A. Detecting triple systems with gravitational wave observations. *Astrophys. J.* **834**, 200 (2017).
51. Rubbo, L. J., Holley-Bockelmann, K. & Finn, L. S. Event rate for extreme mass ratio burst signals in the laser interferometer space antenna band. *Astrophys. J. Lett.* **649**, L25–L28 (2006).
52. Hopman, C., Freitag, M. & Larson, S. L. Gravitational wave bursts from the Galactic massive black hole. *Mon. Not. R. Astron. Soc.* **378**, 129–136 (2007).
53. Toonen, S., Hopman, C. & Freitag, M. The gravitational wave background from star-massive black hole fly-bys. *Mon. Not. R. Astron. Soc.* **398**, 1228–1234 (2009).
54. Berry, C. P. L. & Gair, J. R. Expectations for extreme-mass-ratio bursts from the Galactic Centre. *Mon. Not. R. Astron. Soc.* **435**, 3521–3540 (2013).
55. Amaro-Seoane, P. & Santamara, L. Detection of IMBHs with ground-based gravitational wave observatories: a biography of a binary of black holes, from birth to death. *Astrophys. J.* **722**, 1197–1206 (2010).
56. Sesana, A. Prospects for multiband gravitational-wave astronomy after GW150914. *Phys. Rev. Lett.* **116**, 231102 (2016).

57. Chen, X., Li, S. & Cao, Z. Mass-redshift degeneracy for gravitational-wave sources in the vicinity of a supermassive black hole. Preprint at http://arxiv.org/abs/1703.10543 (2017).
58. Centrella, J., Baker, J. G., Kelly, B. J. & van Meter, J. R. Black-hole binaries, gravitational waves, and numerical relativity. *Rev. Mod. Phys.* **82**, 3069–3119 (2010).
59. Han, W.-B. & Chen, X. Identify binary extreme-mass-ratio inspirals with multi-band gravitational-wave observations. Preprint at http://arxiv.org/abs/1801.07060 (2018).

Acknowledgements

This work is supported by NSFC Nos. U1431120, 11773059, 11690023; the "985 Project" of Peking University, and partly by the Strategic Priority Research Program of the Chinese Academy of Sciences, Grant nos. XDB23040100, XDB23010200, and by Key Research Program of Frontier Sciences, CAS, No. QYZDB-SSW-SYS016. W. H. is also supported by the Youth Innovation Promotion Association of CAS. The authors also thank Pau Amaro-Seoane and Carlos Sopuerta for organizing the 2017 Astro-GR Meeting@Barcelona, where the idea of this work was conceived.

Author contributions

The two authors contributed equally to the idea of this project. X.C. carried out the numerical simulations and wrote the first draft. W.B.H. investigated the probability of detection. Both authors contributed to the text.

Additional information

Competing Interests: The authors declare no competing interests.